Department of Earth science at the University of Iceland

BS-research project (10 Ects), Spring 2009

Relationship between seismic and gravity anomalies at Krafla volcano, North Iceland

Supervisor: Magnús Tumi Guðmundsson

Hélène Le Mével

University of Nantes, France

Contents

1. INTRODUCTION

Iceland is an emerged part of a divergent plate boundary, the mid-Atlantic ridge and situated on a hotspot, region of unusually intense and persistent volcanism (Bransdóttir *et al.,* 2008). This location makes it a unique place to observe mechanisms resulting both from hot spot magmatism and rifting and study the oceanic crust, thanks to refraction crustal studies. In Iceland the plate boundary is expressed through different spreading segments or volcanic systems. A volcanic system is composed of a central volcano and a fissure swarm, usually between 10 km and 100 km long and up to 20 km wide (Arnott and Foulger, 1994). Krafla volcanic system is one of the five NNE-SSW elongated volcanic systems of the Northern Volcanic Zone, north of the Vatnajökull ice cap (Zeeuw-van Dalfsen *et al.,* 2006). Magma chambers generate gravity and seismic anomalies due to the contrast of density resulting from more or less melted rocks.

This report is the result of a research project, completed during the second semester of my Bachelor degree of Earth Sciences at the University of Iceland. The aim was to study the relation between the seismic anomalies and the gravity anomalies arising from the Krafla volcano. The different velocity-density systematics permit to create a density model from the seismic model using the Gravmag software. The existing literature on the crustal structure of Iceland and particularly under the Krafla central volcano gives useful constraints for the model. Different models of the crust beneath Krafla volcano are constructed, gravity anomalies generated, and the results interpreted.

2. KRAFLA VOLCANO: GEOLOGICAL SETTING

2.1. Geological overview

Krafla volcanic system is situated en echelon along the plate boundary, being a part of the Northern Volcanic Zone. The transecting NNE fissure swarm associated is about 10 km wide and 100 km long. The central volcano is characterized by gently sloping topographic high – less than 3°, and about 500m in average a.s.l. – with an elliptical caldera in the middle (10x8 km). The caldera has been associated with an eruption producing semi-acidic welded tuff and rhyolite and dacite ridges during the last interglacial period, about 110000 years ago (Árnason *et al.*, 2008; Sæmundsson, 1979). The whole shield is about 20 km in diameter. The Krafla central volcano is more than 200000years old, and built up from both subglacial and subaerial eruptions (Thordarson and Höskuldsson, 2006); *e.g.* Mt Hágöng and the rhyolite lava domes such as Jörundur were formed during subglacial eruptions.
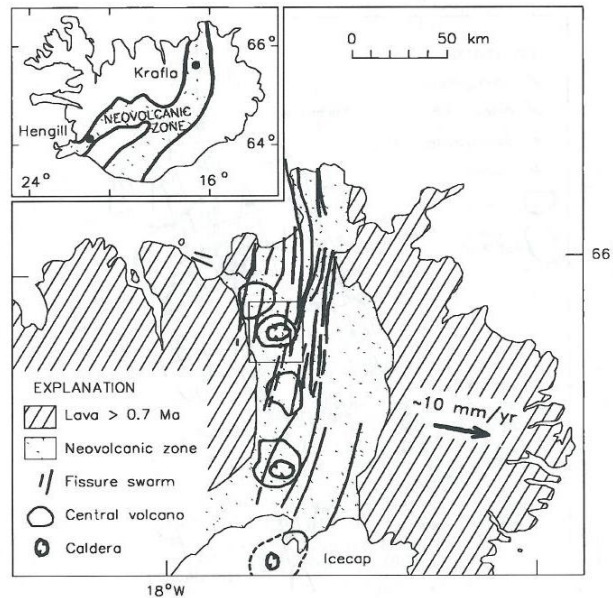
Fig. 2.1. *Simplified tectonic map of NE Iceland, showing the elongated en echelon volcanic systems that characterize the neovolcqnic zone. Arrow indicates the spreading direction; Inset shows the location of the Krafla area within Iceland [from Arnott and Foulger, 1994].*

The caldera is filled with hyaloclastite and subaerial lavas. Below about 1300 m, basalt, dolerite, and gabbroic intrusives are dominant, and below 1800 m a gabbro formation underlies the SE caldera rim (Arnott and Foulger, 1994). A remarkable feature is the presence of sub-alkaline rhyolite around the caldera, which suggests the presence of an underlying magma chamber. Silicic domes and intrusives are present within the caldera as well, probably resulting from the last glacial period volcanic activity. Apart from these exposures, the rocks associated to the Krafla eruptions are mostly basaltic. As an example, during the last eruption in September 1984 a long volcanic fissure produced a pahoehoe lava field of 24 km^2 (Zeuw-van Dalfsen, 2006).

Like many central volcanoes of Iceland, high-temperature geothermal areas are associated. Krafla-Leirhnjúkur geothermal field is inside the Krafla caldera whereas Námafjall geothermal area is located 5 km to the south of the caldera. They are two intensely geothermally altered ridges. Thanks to their exploitation, particularly for electric power generation, Krafla volcanic system is a well-studied area in Iceland.

Krafla is an active volcano and its activity is characterized by rifting episodes and periods of dormancy. It has recently known two main rifting events. The first volcanotectonic episode, from 1724 to 1729 was called "Myvatn fires", during which the crater Víti was formed. 13 km of volcanic fissures formed during this event. The second one, from 1974 to 1985 consisted of long periods of inflation, during which magma accumulated at a shallow depth within the caldera region, and short deflation periods when the magma was intruded laterally into the associated fissure swarm or was erupted at the surface (Brandsdóttir *et al.*, 1997). These 21 rifting events are known as the "Krafla fires" due to the impressive basaltic fissure eruptions. Dikes and lava flows were consequently formed and widened the central part of the fissure swarm; the total widening of the Krafla fissure swarm was in the order of 900 cm and the widening during the Myvatn fires was of the same magnitude (Thordarsson and Höskuldsson, 2006).

4

Since the end of the last tectonic event in 1984, mainly geothermal seismicity occurs in both areas, consisting of continuous and shallow seismic activity. It is therefore limited to the 0-3 km depth interval within the boiling zone of the hydrothermal system (Arnott and Foulger, 1994).

## 2.2   Location of the profile

The profile has been chosen to coincide with the FIRE refraction profile done previously. It is oriented EW and goes approximately from Eyjafjörður to Reydarfjörður. Thus it crosses the caldera *(fig. 5.1; fig. 5.3)* and extends well beyond the caldera rims so that it allows the determination of the different structures at depth beneath the Krafla volcano.

The first point is situated at 65.97°N latitude and -18.01°W longitude. The end point is located 65.55°N and -15.69°W. The studied profile is 115.5km long *(cf. Appendix for the table of data)*.

## 3. USE OF GEOPHYSICAL DATA TO CONSTRAIN MAGMA CHAMBERS

The geophysical techniques are based on detecting differences in physical properties between solid and partially molten rock. A decrease in density and seismic velocity, and an increase in seismic attenuation and electrical conductivity are associated to the presence of a magma chamber.

Indeed, shear waves cannot propagate through a completely molten layer and are attenuated very rapidly in regions of partial melt. For instance, strong attenuation of shear waves from regional earthquakes, interpreted as a diffraction effect, has been used to model magma chambers in Alaska, Kamchatka, Iceland, and New Zealand (Iyer, 1984). In the Kilauea volcano, Hawaii, mapping seismicity patterns in the upper crust has enabled the modelling of the complex magma conduits in the crust and upper mantle (Iyer, 1984).. Active (controlled sources) and passive (local and regional earthquakes) seismic techniques delineate shape of partly melted zone. Thanks to local Earthquake Tomography the 3D structure of the crust can be determined in seismogenic areas down to several kilometers depth, as shown Arnott and Foulger (1994) velocity model. At Krafla volcano, the S-wave shadows confirm the depth of 2-3km for the magma chamber.
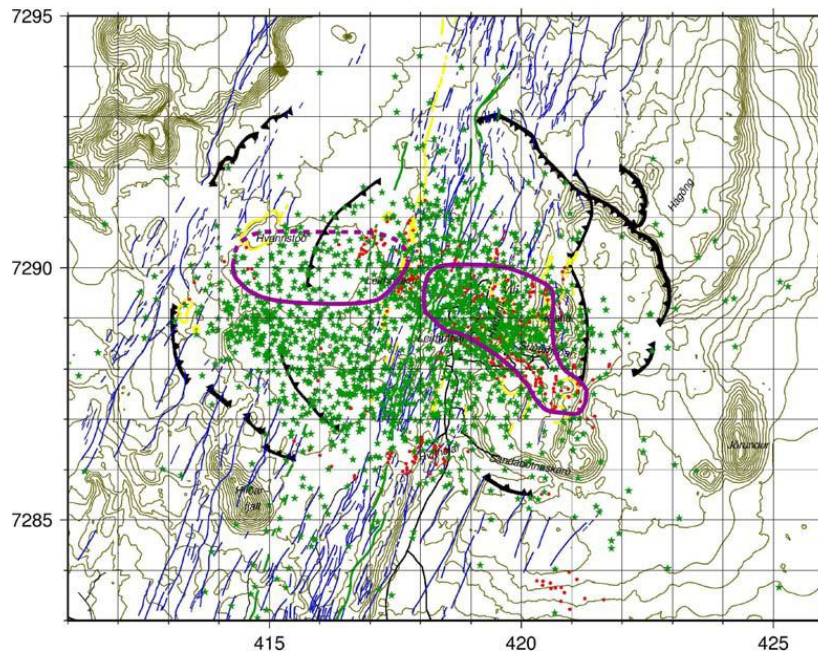
Fig. 3.1. Earthquake epicenters (green stars) and boundaries of S-wave shadows (purple lines) observed during the Krafla fires (reproduced from Einarsson, 1991). Other geological features are the same as on fig. 5.1. [from Árnason et al., 2008].

Electromagnetic methods bring constraints on the thermal structure. Subsurface configuration is also known thanks to resistivity measurements for example MT soundings. MT methods, has shown the resistivity structure of Krafla volcano which delineate the magma chamber.
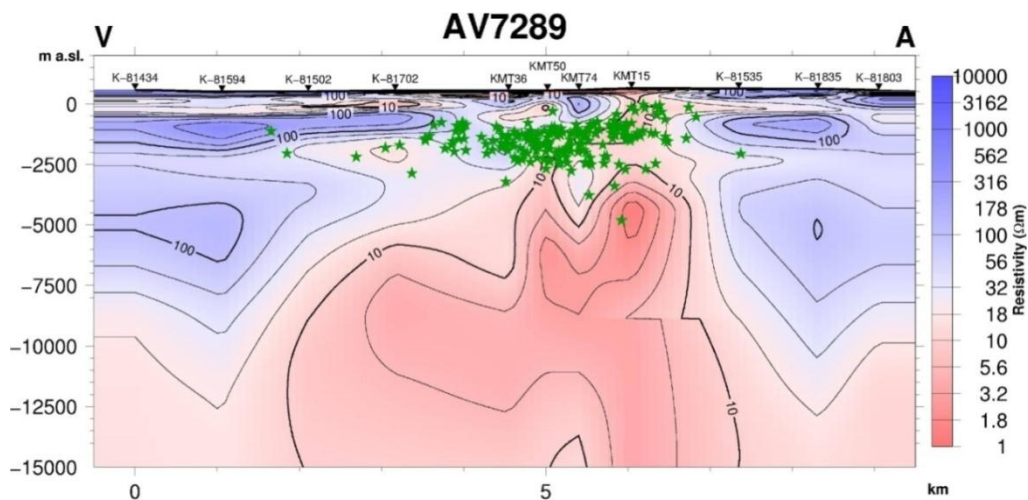
Fig. 3.2. Deep structure of Krafla by MT soundings: low resistivity cap, high resistivity core and a deep low resistivity layer, possibly the magma chamber. Green stars: hypocenters of earthquakes in the roof of the magma chamber, at distances less than 500m. [from Árnason et al., 2008].

Krafla volcano has been extensively studied with different geophysical methods such as INSAR data and micro-gravity data by Zeeuw-van Dalfsen (2006). Microgravity is used to detect inflation or deflation of the volcano. Now it is deflating (gravity decrease due to drainage) but will probably within hundreds of years erupt again. Processes operating at Krafla today: even if it is deflating, krafla system is still subject to deformation, because of stresses associated with the divergent plate boundary, the effects of magma movements and geothermal processes (Zeeuw 2006) which is cooling the volcanic system. Levelling, tilt and GPS observations agree with these observations

Finally, examples have shown that several studies in different tectonic and volcanic environments, which use a suite of geophysical experiments capable of measuring different physical properties of rocks and having a wide range of resolutions, are needed to understand the problems of magma generation, migration, and storage (Iyer, 1984).

4. SEISMIC DATA

The shallow magma chambers of Iceland are identified because they cause local zones of intense shear wave attenuation and delayed P-wave arrival times. Often they are underlain by seismically-fast domes thought to represent gabbroic cumulates (Brandsdóttir *et al.*, 2008). As for the moho, it is defined thanks to strong P-wave and S-wave reflections.

Seismic data to perform the gravity modeling has been found in the previous crustal studies and seismic surveys. I have used the seismic velocities inferred from three different seismic surveys: the 1991 Tjörnes Fracture Zone experiment (Sturkell *et al.*, 1993), the 1993 Krafla reflection/refraction survey, and the 1994 Krafla undershooting experiment (part of the FIRE) (Staples *et al.*, 1997; Brandsdóttir *et al.*, 1997). The Faroe-Iceland Ridge Experiment (1994) was a combined normal-incidence/wide-angle seismic project conducted in July and August 1994 (Staples *et al.,* 1997). The profile went from the Faroe Islands rift to the Krafla volcano. The results constrained the crustal structure and thickness of Iceland as 19 km under the Northern Volcanic Zone.
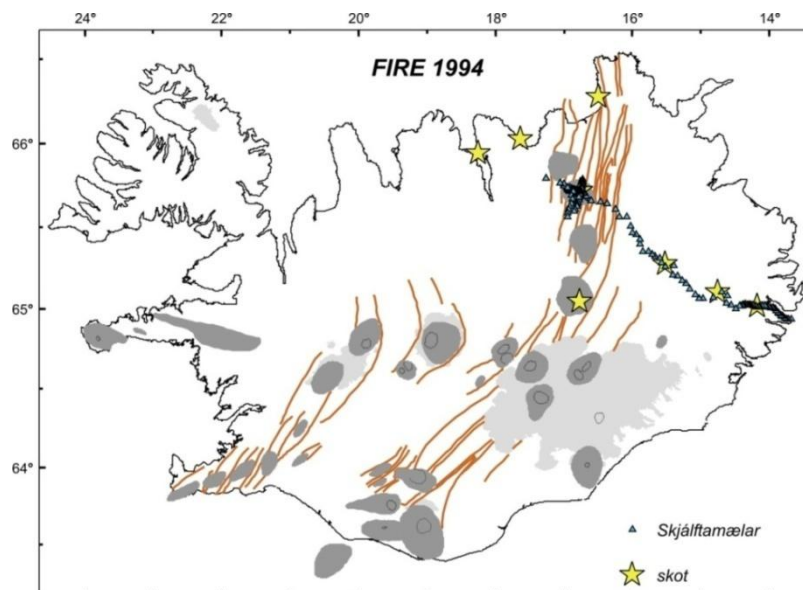

Fig. 4.1. *Map of Iceland showing the seismic stations of the 1994 FIRE line (triangles), shot sites (stars), and earthquakes (squares). [from Brandsdóttir et al., 1997].*

4.1. History of seismic structure of Icelandic crust

Seismological research has been important in Iceland, the main goal being to define the nature of the hotspot, its magma system and its interaction with the mid-ocean ridge. Consequently several seismic surveys have been conducted during the last 30 years and the ideas have evolved. Crustal studies by seismic refraction techniques have been carried out in Iceland since 1959 (Pálmason, 1971).

Bath (1960) made the first refraction experiment in Iceland. He produced a model of the Icelandic crust made of 3 layers and estimated its total thickness to be 28 km. He considered the lowest layer to be part of the crust. Then Tryggvason (1962) used surface wave dispersion analysis to divide the Icelandic crust into a 10 km thick, two-layer stack overlying a half-space (Brandsdóttir *et al.*, 2008) with a P-wave velocity of 7.4 km/s which he concluded represented anomalously low-velocity mantle.

In 1963 and then 1971, Pálmason gave a detailed description of the seismic structure of the crust in Iceland to a depth of about 20 km. He presented a 5 layers crustal structure for Iceland, from the results of 80 refraction profiles in most parts of Iceland. The shallowest seismic layer 0 is a surface layer found only in the neo-volcanic zone (Pálmason, 1971). Its average velocity is $V_p=2.75$ km/s and it is 0-1 km thick. Densities in this layer are highly variable like the P-wave velocity. Layer 1 is about 1.04 km thick and has a velocity $V_p=4.14$ km/s. Layer 2 has the velocity $V_p=5.08$ km/s and is 2.15 km thick. Both layers are mainly tertiary flood basalts (Palmason, 1971). Layer 3 has the velocity $V_p=6,5$ km/s and is 4 to 7 km thick except in northern Iceland where it reaches 12 to 13 km. This layer has an approximately constant velocity. Walker (1975) postulated that layer 3 is a swarm of basic intrusive sheets. Because they penetrated higher into the crust in regions with relatively low density rocks such as hyaloclastites, this layer is found at shallow depth near volcanic centers.
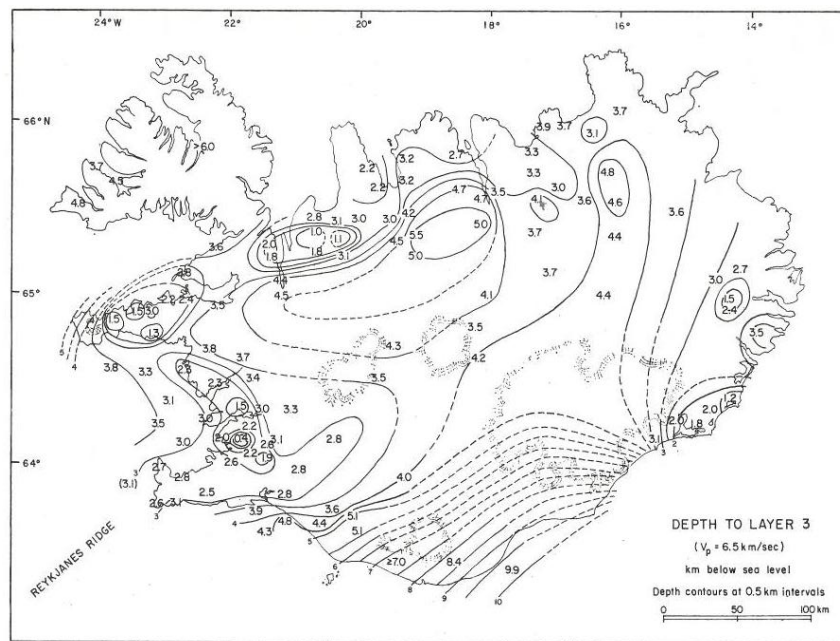
Fig. 4.2. Depth to layer 3 in Iceland according to Pálmason (1971).

From the map, the depth to layer 3 at Krafla volcano is estimated to be about 4 km; we will therefore use this value when constructing the model. Layer 4 has an average velocity $V_p=7.19$ km/s and its depth would vary from 8 to 16 km. However it is not known in northern and eastern Iceland and considerably affected by dips (Pálmason, 1971). The reason for the inaccurate information about layer 4 is the restricted length of his refraction profiles and the smaller number of profiles showing the P_4-wave as compared to the number of profiles showing layers up to layer 3. For Pálmason, layer 4 is anomalous (low-velocity) mantle. He inferred a crustal thickness of 40-60 km beneath Iceland.

Polemic lasted long about the nature of the layer 4 of Pálmason whether it is anomalous mantle material affected by high temperature or high velocity basal oceanic crustal layers (observed by

Stutton *et al.*, 1971). For instance, Angenheister et al. (1979) and Gebrande et al. (1980) developed a model of the crust-mantle transition, favoring a thin crust/hot mantle seismic structure. Tryggvason (1964) also favored a thin crust (10-15km) and a partially molten mantle. However, Angenheister *et al.* (1980) reinterepreted the RRISP shots and indicated a crustal thickness of 30km under Iceland. Bjarnason *et al.* (1993), Staples *et al.* (1997), and Menke *et al.* (1996) interepreted velocities higher than 7 km/s as lower crustal velocities.

Flovenz (1980) reinterpreted Pálmason (1971) data and distincted 2 regions: the upper section in which velocity increases continuously with depth from 2 to 6.5km (layer 1 and 2) and the lower region with nearly constant velocity (layer 3) of 6.5 km/s.

Christensen and Wilkens (1982) studied the composition of the lower Icelandic crust. They noticed a lower velocity for layer 3, large scale fracturing, and elevated temperature. The alteration and epidote content increasing with depth, they assumed the layer2-layer3 boundary is metamorphic and corresponds to the greenschist-amphibolite facies boundary.

Finally, the detection of Moho reflections (P_mP and S_mS) helped to determine whether the crust was thin or thick. It is 11 km thick at the Reykjanes ridge, 21 km in southwest Iceland and there is a marked crustal thickening towards the center of the Iceland plume (Brandsdóttir *et al.,* 2008).
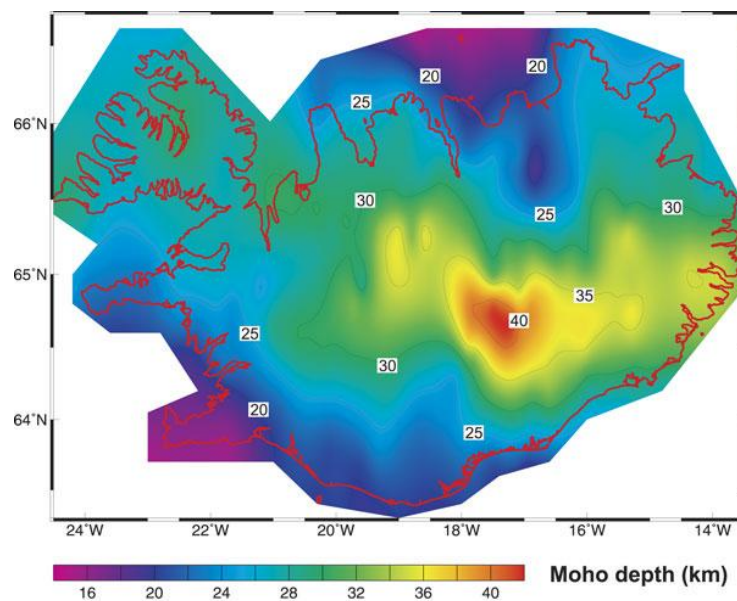
Fig. 4.3. *Map of total crustal thickness determined using a combination of explosion seismology profiles and gravity [from Darbyshire et al., 2000].*

Iceland crustal structure is comparable to oceanic crust but is unique on different points. It has a much greater thickness (3-5 times thicker) being 20 to 40 km thick and is dotted by high-velocity upper crustal domes beneath the eruptive centers (Brandsdóttir *et al.*, 2008). Moreover, it has permanent, small, shallow magma chambers. Large variations affect the upper crustal velocities from 0 to 15 km and the lower crustal velocities are more uniform.

4.2. Different contributions to the crustal structure model of Krafla

The shallow crustal Krafla magma chamber has first been detected after the rifting episode of 1975 (Brandsdóttir *et al.,* 2008). Einarsson (1978) was the first to delineate two regions of high shear wave

attenuation. He used local earthquakes recorded during an inflation period. His assumption was the presence of a shallow crustal magma reservoir, situated at approximately 3 km depth. This magma chamber is about 2 km by 7 km and divided near its top. He constrained the lower boundary of the magma chamber to 7 km depth maximum.

Ármannsson et al. (1987) provided information concerning the lithology and tectonics of the Krafla-Leirhnjúkur geothermal field. He divided the subsurface formations between: an upper, extrusive section and a lower, intrusive section (Brandsdóttir *et al.*, 1997). The seismic structure of the uppermost 2 km of the caldera is relatively flat-lying.

Brandsdóttir and Menke (1992) inferred the thickness of the magma chamber from waveform studies on earthquakes from the Krafla caldera during the July 1988 inflation period. They constrained it to less than 1km thick.

Arnott and Foulger (1994) created a 3D velocity model of Krafla, using local earthquakes and artificial sources recorded at a local array of seismic stations. The main characteristics outlined by this model are the strong lateral heterogeneities, and the high-velocity bodies. They are located around the caldera rim and are assumed to be shallow crystalline intrusives. It turned out that they overestimated the amount of lateral heterogeneity in the upper 2 km of Krafla caldera (Brandsdóttir *et al.*, 1997). They also suggested that the magma chamber is divided into two lobes in its upper part (Arnott and Foulger, 1994).

Brandsdóttir *et al.* (1997) created a velocity model across the Krafla volcano from the interpretation of the FIRE data. They found two P-wave shadow zones within the Krafla caldera which are caused by thin, flat-lying low-velocity layers at 1300 and 1700m below the surface of the caldera (to the west of the Víti crater). Because they do not show strong shear wave attenuation, they do not represent magma. It is probably due to high porosity in the basaltic intrusive and is related to geothermal aquifers. Seismic velocity structure at Krafla is characterized by large variations in compressional velocity (Brandsdóttir *et al.,* 1997). The near-surface structure is approximately flat-lying (*fig.4.4-4.5.)* with only minor lateral heterogeneities. The moho rises from 25 km depth at the western edge of the NVZ, to 19 km beneath Krafla and then descends to 35 km depth in eastern Iceland (Brandsdóttir *et al.,*1997).
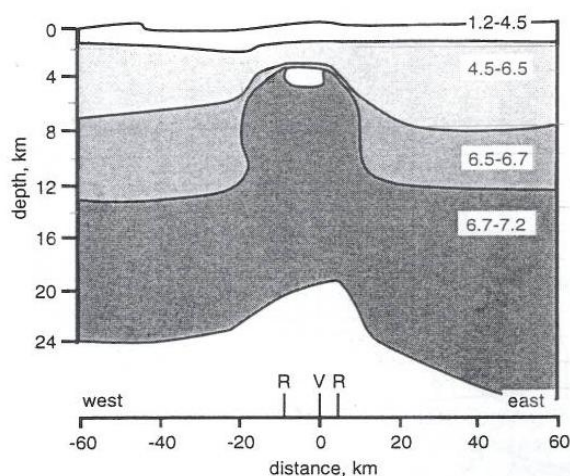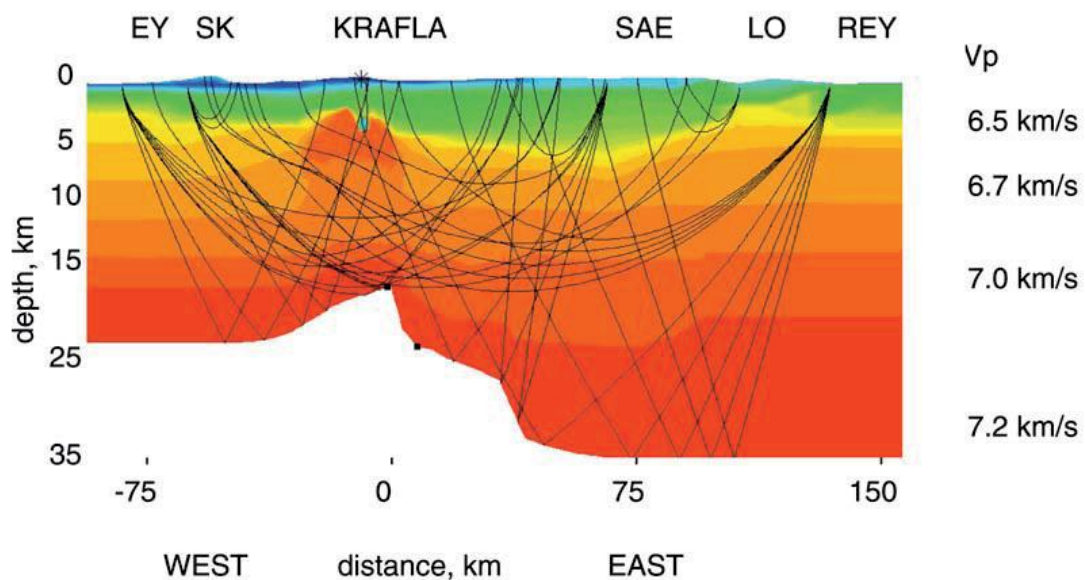

Fig. 4.4. *Crustal structure of the Krafla central volcano. A two-dimensional, compressional velocity model derived from travel time data from the E-W profile, structure across the plate boundary. The shaded refion on top of the high-velocity dome denotes the magma chamber. [from Brandsdóttir et al., 1997].*
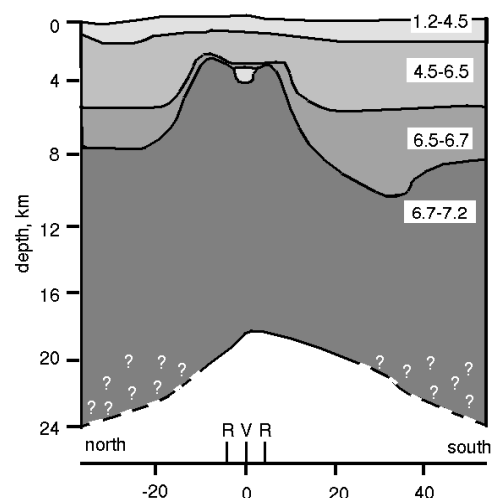
Fig. 4.5. *2D model of the compressional velocity structure of Krafla volcano, along the plate boundary. The rims of the caldera are labeled R, the position of the magma chamber, V. Only the part of the N-S model beneath the central volcano itself is well-resolved as the length of the N-S profile is only 22km. [from Brandsdóttir et al., 1997].*

Doming of the lower crust is observed beneath the Krafla central volcano. It consists of olivine-rich cumulates, formed at the base of the magma chamber and advected downward and outward during the spreading process (Menke and Sparks, 1995; Brandsdóttir *et al.*, 2008). The high velocity dome is 33 km wide, extends from 11-14 km depth in the lower crust and is narrowing upward *(fig. 4.4 and 4.5).* The 6.5 km/s isovelocity surface (Pálmason layer 3) rises up to 2.6 km depth. The Krafla dome may be at least 1.8 million years old according to its size and on the half-spreading rate of 0.9 cm/year (Brandsdóttir *et al.,* 1997).

The magma chamber sits at the top of the dome near 3 km depth. Its size corresponds to the size of intense shear wave attenuation: 2-3 km wide in the N-S direction and 8-10 km wide in the E-W direction (Brandsdóttir *et al.*, 1997) which implies an oblong shape, as determined Einarsson in 1978. Its thickness is 0.75-1.8 km assuming that the magma velocity is 3 km/s and the background velocity is 5-6 km/s. Its volume is therefore 12-54 km^3, assuming a tabular shape (Brandsdóttir *et al.,* 1997).


Fig. 4.4. *Crustal structure across the Krafla volcanic system along the FIRE refraction profile, NE-Iceland, adapted from Brandsdóttir et al. (1997). [from Brandsdóttir et al., 2008].*

4.3. P-wave-velocity-density systematics

Studies showed a consistent relationship between both shear and compressional velocity and wet bulk density. The approach is to convert the velocity to density, to calculate the simulated Bouguer anomaly field, and then compared with the observed Bouguer anomaly field calculated from the gravity data. In this project we will consider 3 velocity-density relationships, appropriate for oceanic basalts.

Pálmason (1971) as seen previously (*cf. part 4.1.)* presented a model of the oceanic crust in 5 layers.
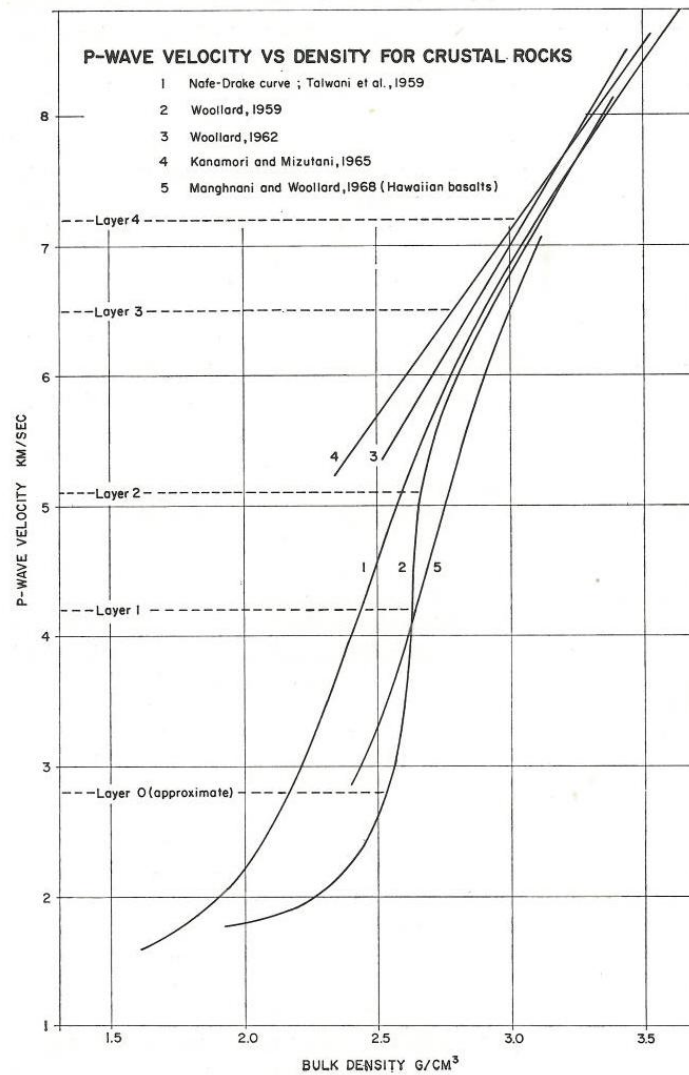
Fig. 4.5. *P-wave velocity density curves for crustal rocks. [From Pálmason, 1971].*

The above graph shows that there is a good agreement between authors for velocities above 7 km/s but the relations differ for lower velocities. From this graph Pálmason (1971) estimated the most probable densities for each layers.

Layer	Average P-velocity (km/s)	Average density (Mg/m^3)	Average thickness (km)
0	2,8	2,1-2,5	0-1
1	4,2	2,6	1,04
2	5,1	2,65	2,15
3	6,5	2,9	4-7
4	7,2	3,1	?

Table 1. *Average P-wave velocity, density and thickness for oceanic layer [from Pálmason, 1971].*

Christensen and Wilkens (1982) made measurements of compressional and shear wave velocities, densities and porosities from measurements in the Reydarfjörður drillholes in Eastern Iceland. They deduced a relationship with alteration and porosity. The measurements of velocities have been made from flow basalts and dikes at a pressure of 1 kbar.
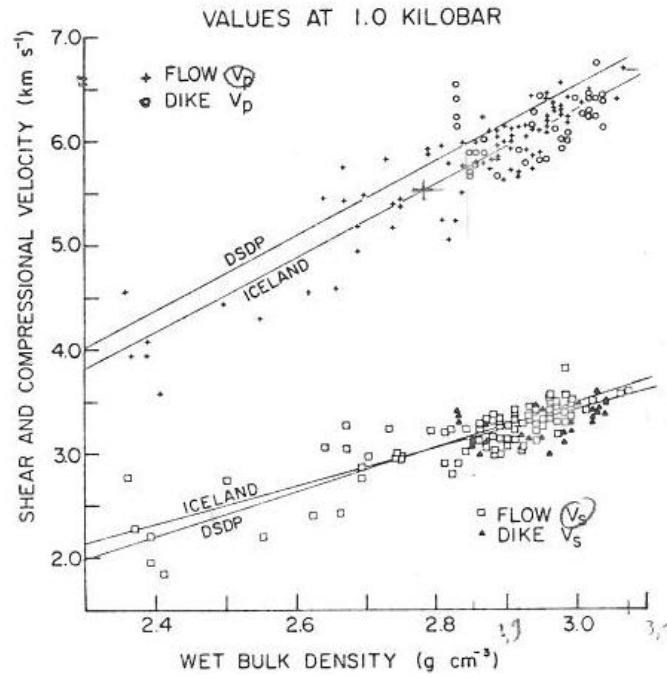
Fig. 4.6. *Shear and compressional velocity versus wet bulk density.Linear fits for Iceland (from Christensen and Wilkens, 1982) and DSDP basalts (from Christensen and Salisbury, 1975).*

For a given density, the bulk of Iceland samples has slower compressional velocities than DSDP (Deep Sea Drilling Project) basalts. One explanation could be the effect of iron; indeed, iron rich samples have slower velocities. The presence of quartz in Icelandic sample would influence this relation as well. Porosity is the controlling factor in the bulk density (Christensen and Wilkens, 1982) so there is a systematic relationship between porosity and velocity. In this study I chose the following linear regression equation for Iceland:

$$\rho = 1{,}53 + 0{,}230 V_p \tag{4.1}$$

where V_p is the P-wave velocity (km/s) and ρ is the rock density (Mg/m^3).

Carlson and Herrick (1990) studied densities and porosities of oceanic crust using results from drilling and downhole logging. They found empirical relationships between in situ densities, porosities and seismic velocities for the oceanic crust. For the region of the crustal velocity model with velocities smaller than 6.7 km/s, we use the relationship between V_p (km/s) and ρ (g/cm^3):

$$\rho = 3{,}81 - 6{,}00 / V_p \tag{4.2}$$

For velocities greater than 6.7 km/s, the relationship is the one calculated from gabbro and diabase samples (Carlson and Herrick, 1990):

$$\rho = 5{,}23 - 15{,}38 / V_p \tag{4.3}$$
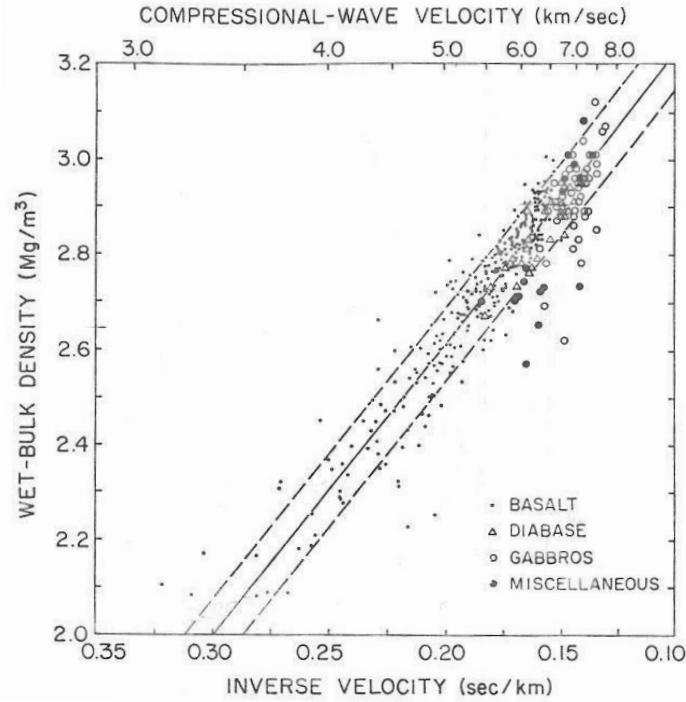
Fig. 4.7. *Wet-bulk density versus P-wave slowness in laboratory samples from ophiolites and from the upper oceanic crust. Velocities were measured at 40MPa confining pressures under water-saturated conditions. "Miscellaneous" includes rock types such as serpentinites and amphibolites which are present but not abundant in the oceanic crust. Solid line isbest fit of density on slowness; dashed lines represent rms error. [from Carlson and Raskin, 1984] (in Carlson and Herrick, 1990).*
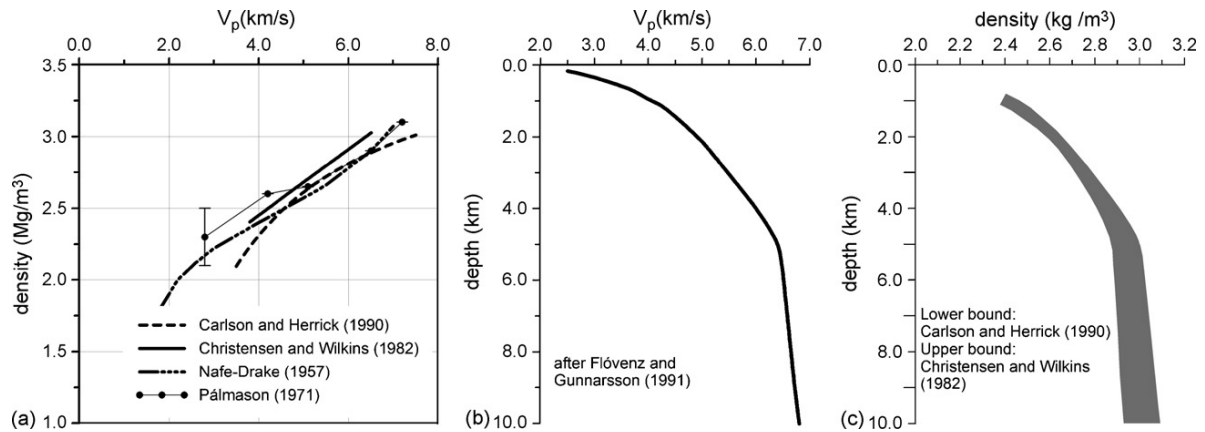
Fig. 4.8. *(a) Comparison between the different Density-P-wave velocity systematics (Narlson and Herrick, 1990). (b) The velocity-depth profile down to 10km depth for uneroded Icelandic crust (Flovenz and Gunnarsson, 1991). (c) The most likely density-depth profile of the Icelandic crust based on the velocity-density systematic. The two models of Carlson and Herrick (1990) for oceanic crust and Christensen and Wilkens (1982) provide respectively the lower and upper bound for the density profile [from Guðmundsson and Högnadóttir, 2007].*

Another equation that is commonly used by exploration geophysicists to relate physical properties and lithology is the Nafe-Drake equation (1963). Nafe and Drake (1963) established an empirical relationship between the P-wave velocity and density of water-saturated sediments and sedimentary rocks. It is commonly used to evaluate the density of sedimentary rocks in shallow seismic surveys. Therefore, we will not consider this systematic in this project.

4.4.   Density of Icelandic rocks

Originally, the Bouguer correction of the early gravity surveys was made using a uniform reduction density (2600 kg/m^3) (Staples *et al.*, 1997). However, lower surface densities have been observed in

Quaternary rocks. Schleusener *et al.* (1976) measured sample densities of 2100-3000 kg/m^3 for quaternary basalt and 1700-2500 kg/m^3 for quaternary hyaloclastite rocks. For the unconsolidated surface layer, 2400 kg/m^3 is found for areas of quaternary surface rock and 2100 kg/m^3 within 10 km of the Víti crater in the Krafla caldera, where hyaloclastite rocks dominate (Staples *et al.,* 1997). It correlates the very low seismic velocities (1,2-2,6 km/s) measured in the uppermost hundred meters of Krafla lava. For the modeling, the surface layer is split in three zones, and three different densities are attributed according to Schleusener *et al.* (1976). From W to E, the tertiary basalt zone, composed of old lava flows, has a mean density of 2.7 Mg/m^3; the central volcanic zone has a density of 2.3 Mg/m^3, and the intermediate zone has a density of 2.5 Mg/m^3.

5. GRAVITY DATA

One of the first gravity surveys of Iceland was made by Einarsson in 1954. Small wavelength anomalies are superimposed on the main anomaly and correspond to volcanic centers. The small amplitude gravity anomalies have in many cases been shown to be related to anomalies in the delay time of the P_3-wave (Pálmason, 1971).

5.1. Bouguer gravity map
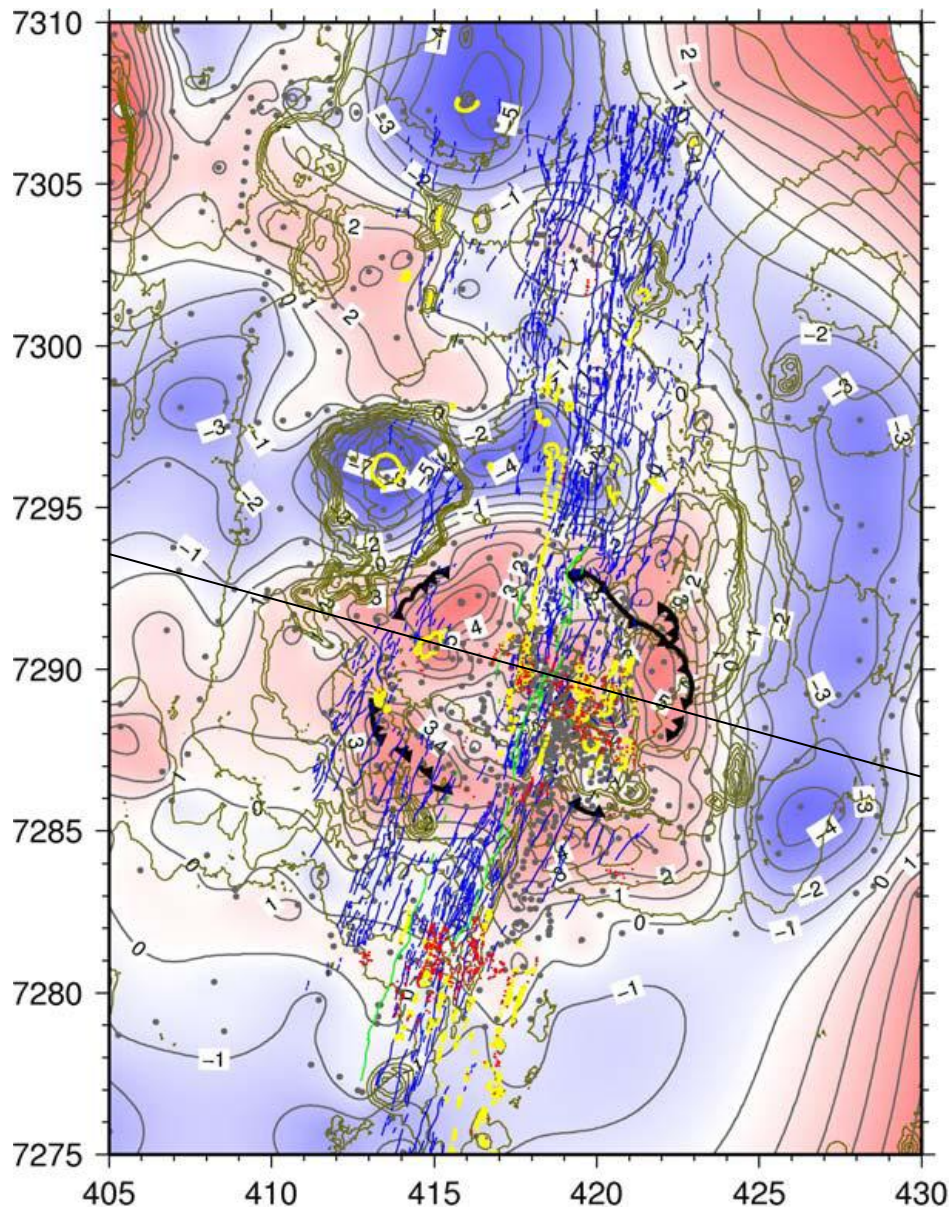
Fig. 5.1. De-trended Bouguer gravity map (mgals) of Krafla and surrounding areas. Geological information: faults and fissures (blue), the caldera (black), eruptive fissures and craters (yellow), geothermal surface manifestations(alteration, hot springs, fumaroles) (red). Boundaries of the part of the fissure swarm that was active in Krafla fires are shown as green lines. [from Arnasson et al., 2008].Central part of the studied profile (black line).

The Bouguer reduction density used for this map was 2.49 g/cm^3. The map has been detrended by subtracting the long wavelength background. The first observation is the gravity high associated with the central volcano (*fig. 5.1*), which is caused by the massive intrusions in the roots of the volcano and its lava shield. Under and to the east of Gæsafjöll there is a distinctive gravity low as well as to the east of Hágöngur. The latter connect to a gravity low along the Húsavík transform fault in the north and thus form a NS trending gravity low (Árnason *et al.,* 2008).

16
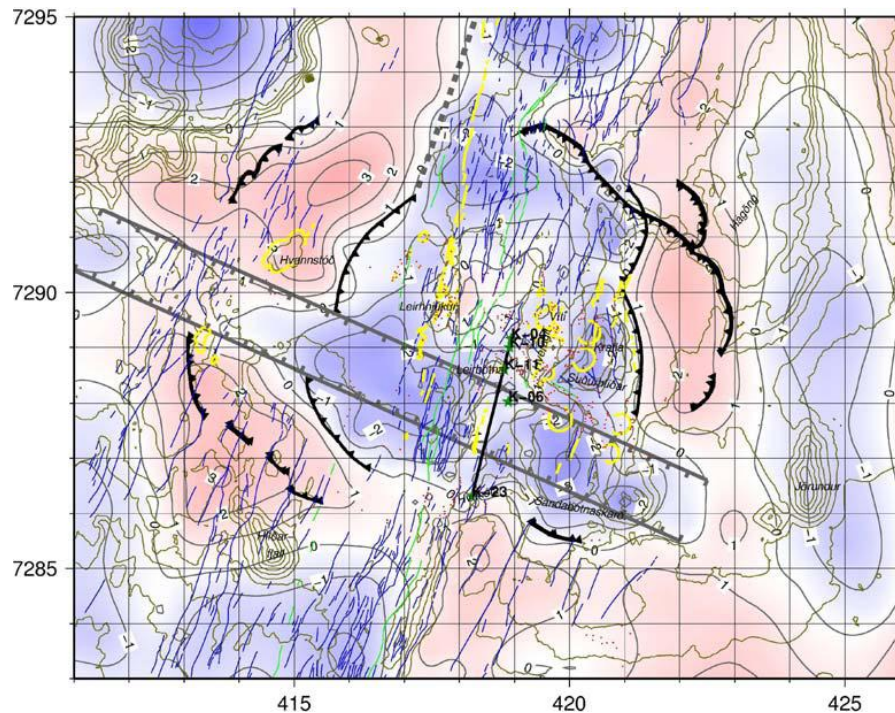
Fig. 5.2. *De-trended Bouguer gravity map (mgals) of Krafla volcano. The rims of the outer caldera and the inferred buried inner caldera are shown (hedged black lines). An inferred ESE-WNW transform graben is shown (gray fault lines). A linear density contrast in the fissure swarm to the north is also shown (gray broken line). (From Árnason et al., 2008).*

Within the caldera (*fig 5.2*) there is a relative gravity low, and surimposed to it is a gravity high at Leirhnjúkur. It could reflect intrusions and the magma chamber. Two linear gravity lows are present in the caldera, and where these anomalies cut through the caldera rim, the rim is not visible.

As seen previously, the caldera is about 110000years old. The spreading rate being about 1.8-2 cm/year, the total spreading of the caldera is about 2 km since its formation (Árnason *et al.,* 2008). Considering that most of the spreading takes place in the fissure swarm through the caldera and that the gaps in the caldera rims are about 3.5 to 4km at the surface, parts of the rims must be subsided and buried. We can also observe gravity highs associated to the caldera rim and surrounded by steep gradient towards the central low. This indicates a density contrast at shallow depth. That could be another caldera buried inside the surface caldera. The inferred buried caldera and the transform graben transecting the outer caldera probably have been filled with hyaloclastite, of lower density. There are evidences for the inferred graben (probably formed between 80000 and 40000 years ago) and dense intrusives from borehole data (Ármannsson *et al.,* 1987).
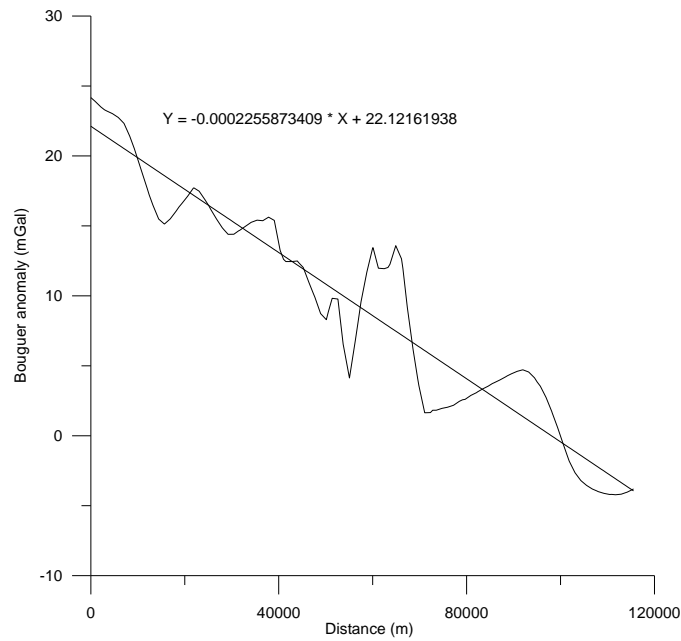
5.2. Gravity profile

Three sets of gravity data have been used. Two concerning the Krafla caldera area and the 3rd one being regional data, selected to fit the area of interest. Data have been given by ISOR Iceland GeoSurvey, from the Bouguer gravity map of Iceland, along the FIRE line east of the neovolcanic zone. They are gravity data collected during an extensive gravity survey from 1976 to 1984 (Johnsen, 1995). Two other sets of gravity data concerning the area nearby the Krafla caldera have been added, given by M.T. Gudmundsson.

Using Surfer software, a grid and contour map have been created and then sliced to obtain the gravity profile.
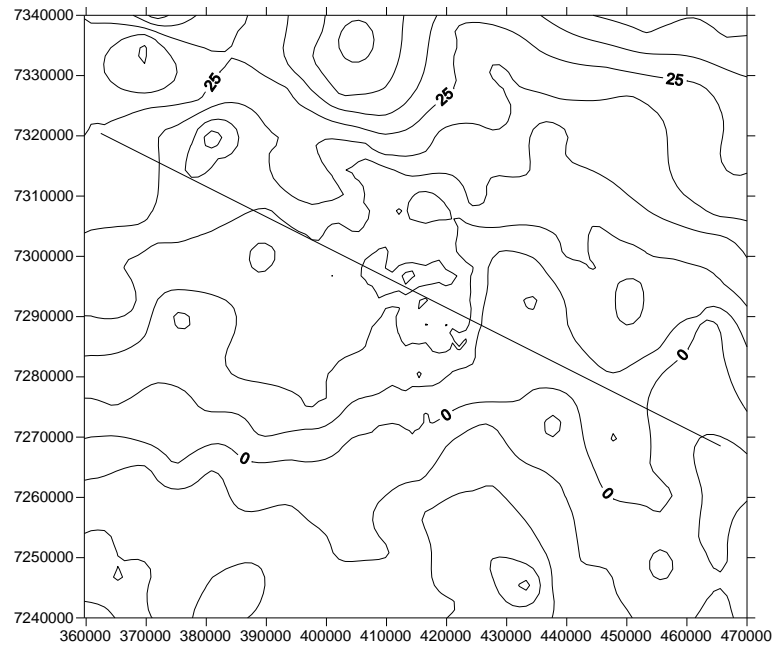
Fig. 5.3*. Contour map of the total gravity field in Krafla area.Bouguer anomaly in mgals.The coordinate system is UTM. Position of the studied profile (black line).*

Fig. 5.4*. Observed gravity field along the profile. The regional field is estimated by a linear trend.*

The regional field observed on *fig. 5.4.* corresponds to the gravity low of Iceland. Our interest being the smaller wavelength anomaly corresponding to the subsurface structure of the Krafla caldera, the regional field has to be removed by a trend analysis. Here, the regional gravity-gradient can be approximate by a linear curve. It is then subtracted to the observed data and the positive or negative residual anomalies can be interpreted.
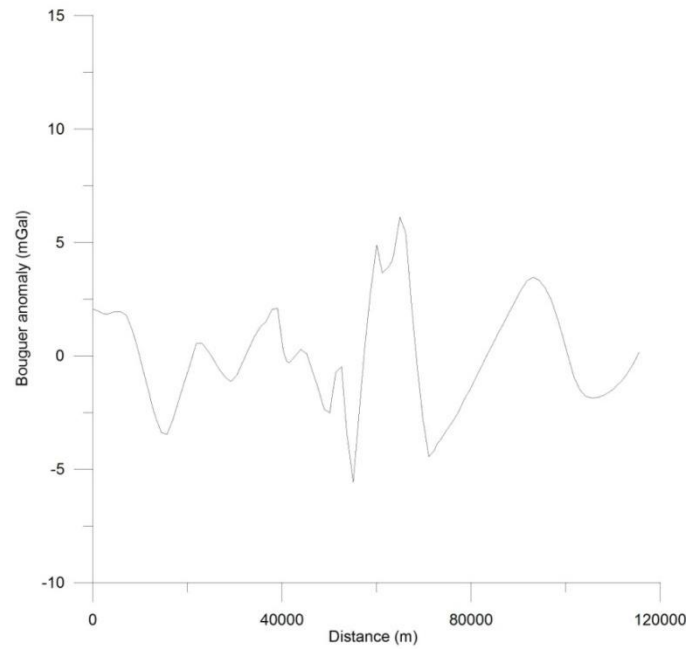
Fig. 5.5. *Residual gravity anomalies (mgals) across Krafla caldera, after removal of the regional field.*

5.3.   Interpretation of gravity anomalies and forward modeling

Any given anomaly could be caused by an infinite number of possible sources (Kearey *et al.,* 2002), that is the inverse problem. In this project the aim is to use seismic data and observe the resulting gravity anomalies. Therefore, the possibilities are reduced, and the nature and form of bodies are also used as constraints. Other geological information such as outcrops and boreholes can also be used to restrict the model. The indirect interpretation principle is as follows: the causative body of a gravity anomaly is simulated by a model whose theoretical anomaly can be computed, and the shape of the model is altered until the computed anomaly closely matches the observed anomaly (Kearey *et al.,* 2002). This iterative process gives the best fit with the observed anomaly.

Gravmag software (Pedley *et al.,* 1993) is a modeling program and permits a 2.5D interpretation of gravity data. The model is created out of polygons which are assigned a finite strike length. The strike of the polygons is perpendicular to the profile. The theory for the gravity calculations is taken from Rasmussen and Pederson (1979) (Pedley *et al.*, 1993).

The settings used in Gravmag for the field data file are: "2"=unequally spaced data at separate gravity field stations; "M"= meters; "MG"=mGal; "132"=number of gravity field points; "0"=gravity modeling only; "0"=observation surface at the topography; "0"=no magnetic modeling. The data file parameters are the observed gravity value, the X coordinate for gravity value (distance) and the elevation for each point. The gravity is the residual anomalies (*fig.5.5*) from the 132 points profile. Topography has been obtained by converting then drawing the gravity profile coordinates and estimating for each point the topography from the 1/250000 topographic map of Iceland (*see Appendix for data*). The Universal Transverse Mercator system (UTM) coordinates was converted to geographic coordinates. Iceland is sitting on 3 zones; the eastern part, including Krafla area is in the 28W zone.

6. RESULTS AND INTERPRETATION

10 polygons have been drawn to express the density changes along the profile across the Krafla caldera. They have been delimitated depending of the velocity gradient (used by Brandsdóttir *et al.*, 1997) and have been affected an average density, according to the different systematics. Their shape has been reproduced according to previous seismic refraction profiles. As in the FIRE gravity modeling (Staples *et al.*, 1997), half-widths are used to reproduce the volume of conical features. For polygon 7, a half-width of 5 km will be used for all models, and for the uppermost part of the anomalous mantle, a half-width of 10 km. All other layers are considered as infinite plates so we attribute a large half-strike value (1000km).

A topographic layer is created down to sea level so that the calculated gravity is not influenced by topographic effects. It has first been given the reduction density (2.8 Mg/m^3). Finally it was split in three zones, and three different densities were attributed according to Schleusener *et al.* (1976) (*cf. part 4.4).* Afterwards, these values have been adjusted.

Because seismic and gravity models centers was not centered, the magma chamber anomaly was not coinciding with the observed gravity curve. This comes probably from a mistake in the seismic model, which did not consider the center of their profile as the center of the caldera. I subtracted the difference in distance (*Appendix*) so that both curves could fit.

6.1. Carlson and Herrick (1990) systematic

First the seismic model is drawn, according to Brandsdóttir *et al.* (1997). The average velocity for each layer is chosen to represent the range of velocities (*fig.4.4, 4.5, 4.6*) and equations *(4.2)* and *(4.3)* are used to convert P-velocity to density.
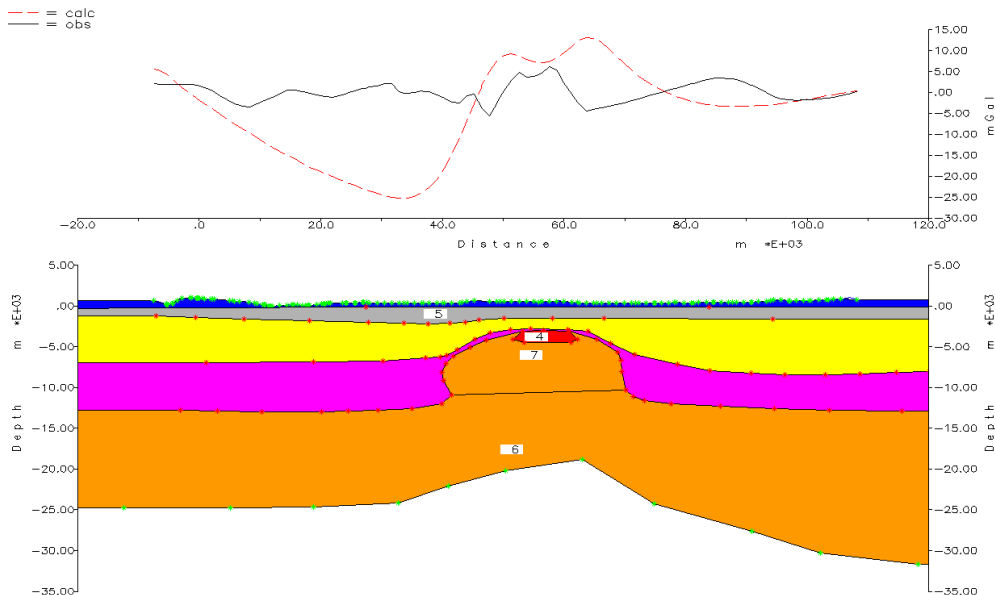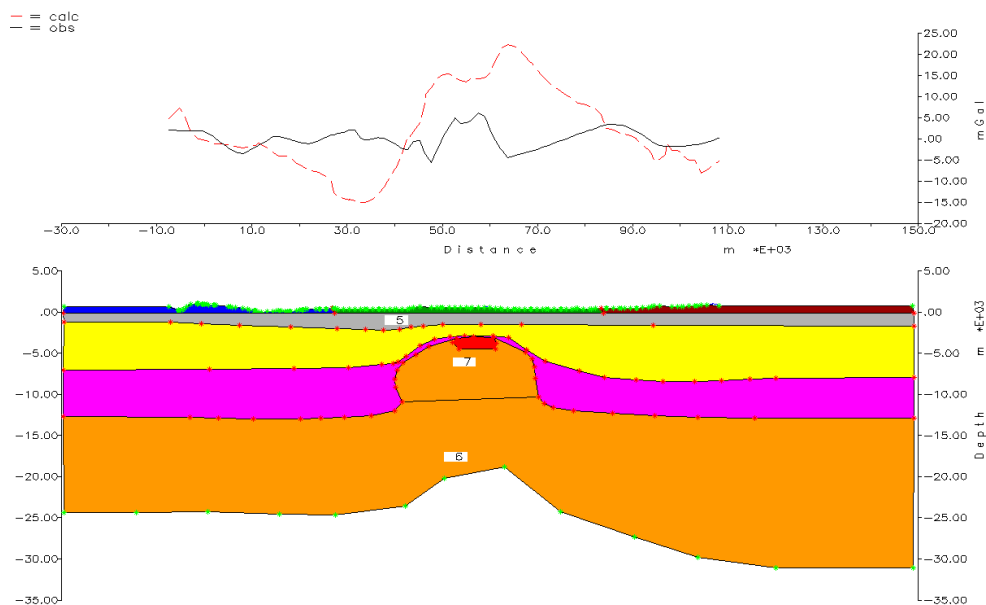

Fig. 6.1. *Forward 2.5-D gravity model 1over Krafla caldera. Properties of the bodies are given in Table 2.*

| Polygon	1	2	3	4	5	6	7	Bckgrd
Density (Mg/m^3)	2.85	2.719	2.901	1.81	1.81	3.017	3.017	2.85

Table 2. Properties attributed to the polygons of the gravity model 1.

This model is not correct. Therefore I divided the topographic layer in three parts. As seen in the geological overview, the caldera is filled with hyaloclastite which explain the lower density in this part of the profile.
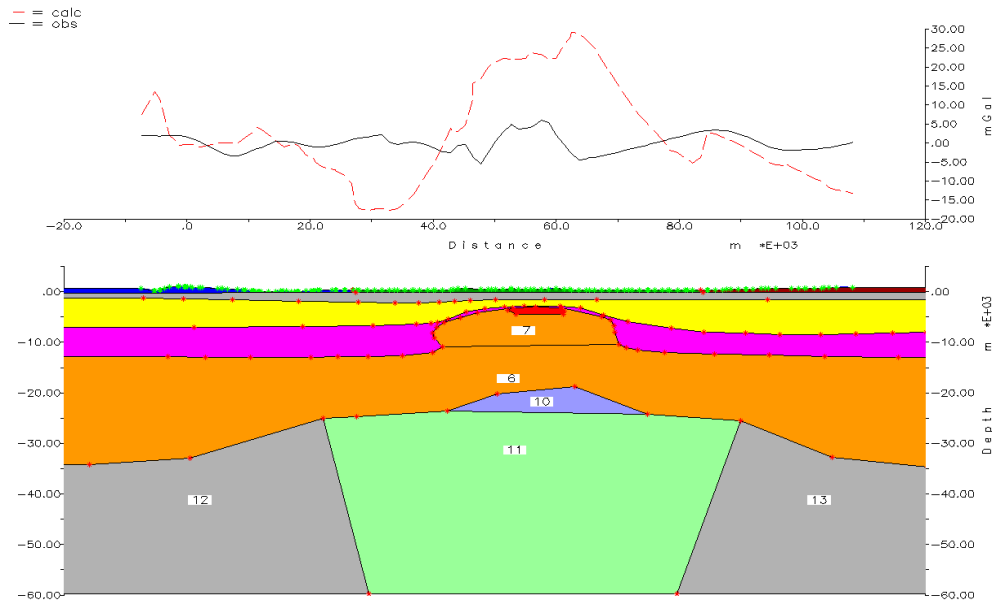

Fig. 6.2. Forward 2.5-D gravity model 2 over Krafla caldera: surface layer split in three zones.

I then corrected for the thickness of the crust. Indeed, Staples *et al.* (1997) indicates a thickness of 35km on each side of the volcanic zone.
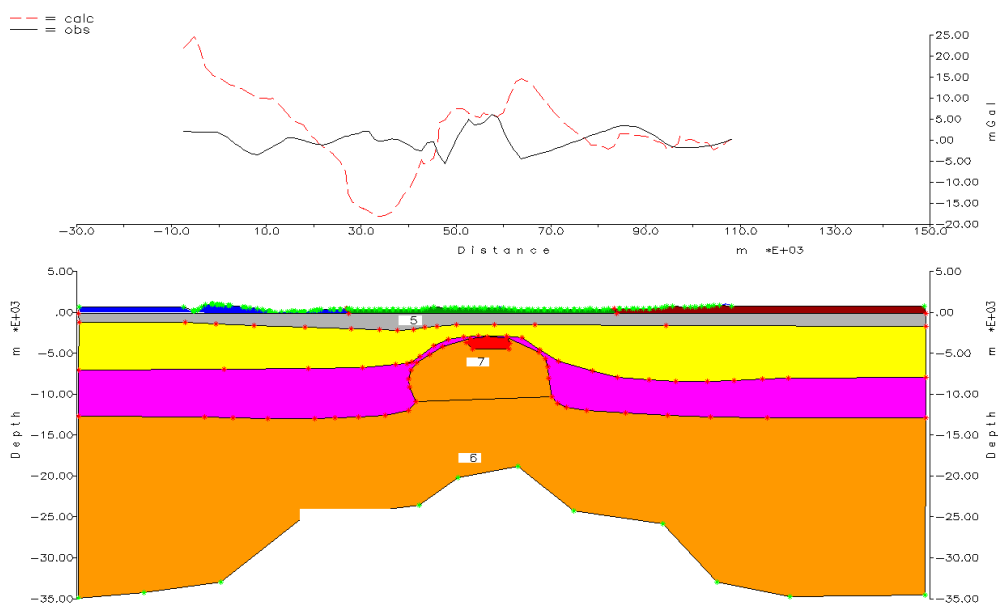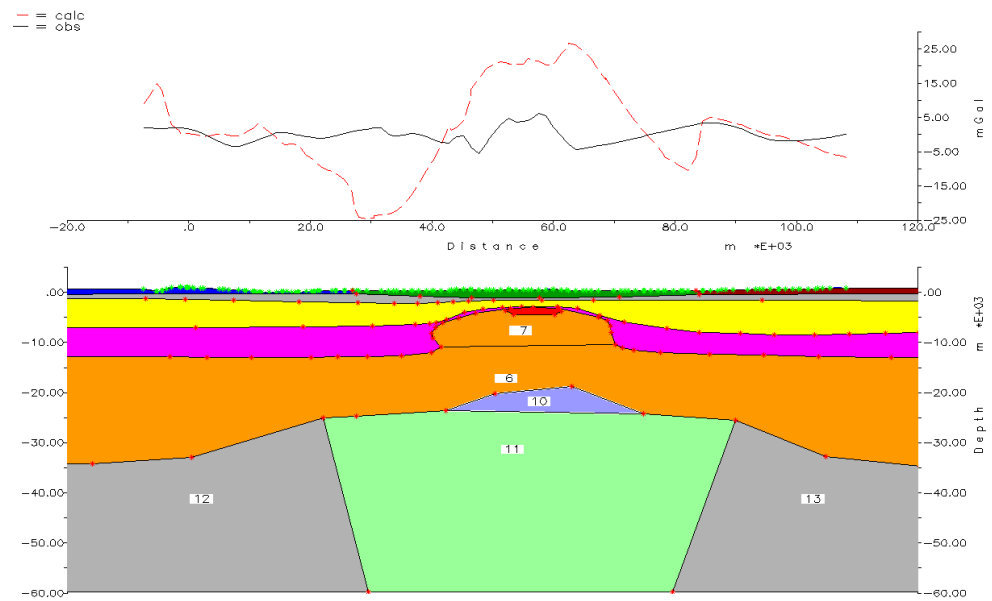

Fig. 6.3. Forward 2.5-D gravity model 3 over Krafla caldera: thicker crust, down to 35km.

It seems that the density of the topographic layer is too high on the left side. Therefore I decided to adjust it and make it to 2.5 Mg/m^3 like the volcanic zone. In model 4, I also added another polygon representing a low-density zone in the mantle (density of 3.17 Mg/m^3) (Staples *et al.*, 1997). After optimization of the property the following densities (in Mg/m^3) have been attributed: $\rho_{12 \& 13}$=3.22, $\rho_{10 \& 11}$=3.05. A background density of 2.99 was necessary to adjust for the higher density of the mantle.
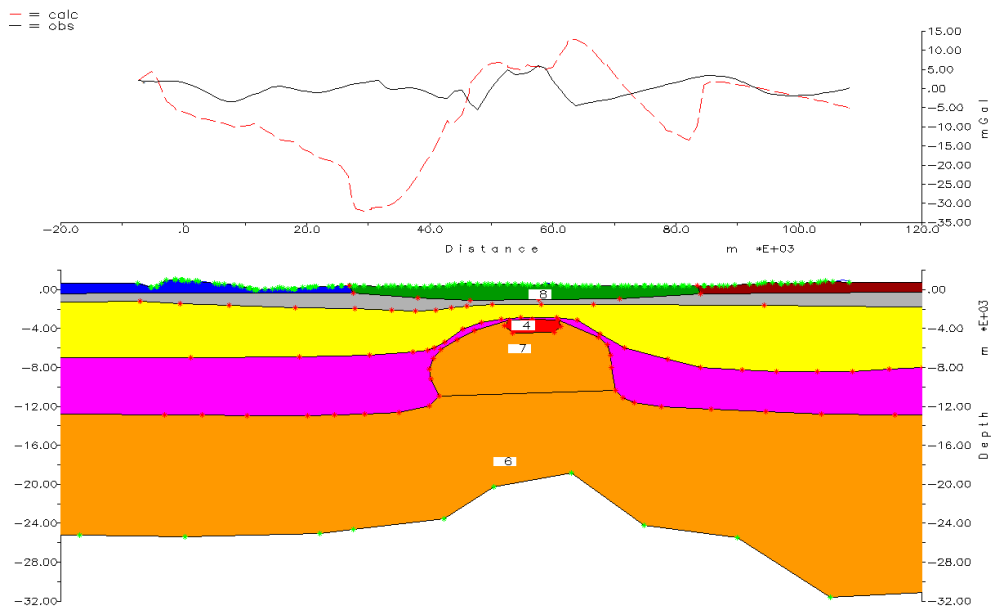

Fig. 6.4. *Forward 2.5-D gravity model 4 over Krafla caldera: presence of anomalous mantle.*

The fit is better but there are still major discrepancies. One possibility is to make the crust above the volcano thicker, to account for the weight of successive lava flows. The crust is made 1 km thicker. For model 5, I attributed the following densities: $\rho_{10 \& 11}$=3.03, $\rho_{12 \& 13}$=3.22, topographic layer: ρ_1=2.7, ρ_8=2.3, ρ_9=2.9 and the background density is 2.99.

Fig. 6.5. *Forward 2.5-D gravity model 5 over Krafla caldera: the central part of the surface layer is 2 km thick.*

The model 6 has the same properties but the mantle is not represented. For the topographic layer the densities are (from left to right): 2.7, 2.28 and 2.87.

Fig. 6.6. *Forward 2.5-D gravity model 6 over Krafla caldera.*

Finally the density of the dome could be reduced but it does not have a significant influence for this gravity model.

Among all these models, the model 5 and 6 are the one which fits the best. The two gravity lows on each side of the main high are created by the boundary between the three zones of the topographic layer. If we do not consider this edge effect, the calculated gravity field approximates the observed one. The densities of the topographic layer had to be corrected form the one found by Schleusener *et al.* (1976). They are still consistent with the actual petrology.

For the next systematics, I successively tried all the combinations above. I present the gravity models with the best fit and the most probable.

6.2.   Pálmason (1971) systematic

The properties of the layers of Pálmason (1971) seismic model are summarized in *table 1.*

Model 1

Layer 0 and 1 are divided in three parts. From left to right the densities (in Mg/m^3) are: 2.606, 1.908, 2.420. Layer 2=2.630; Layer 3=2.9; Layer 4=3.1.
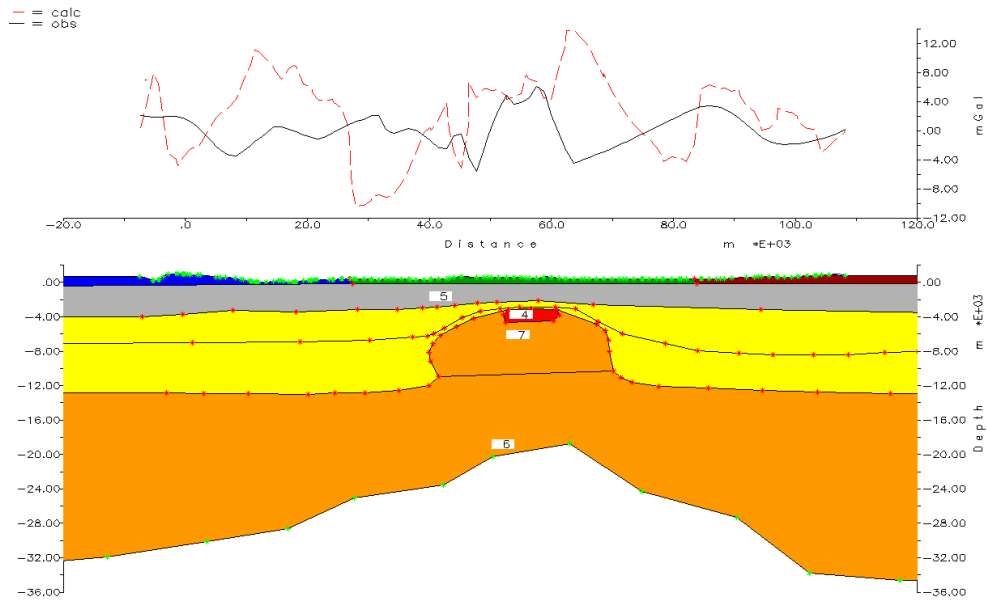
Fig. 6.7. *Forward 2.5-D gravity model 1 over Krafla caldera, according to Pálmason (1971) crustal seismic structure.*

Model 2

Background density: 3.054 Mg/m^3. Layer 0 and 1: 2.688, 2.015, 2.637. Layer 2 and 3 are the same as in model 1. The density of the dome has been lowered to 2.913. The mantle is added: $\rho_{10 \& 11}$=3.108, $\rho_{12\&13}$=3.23.
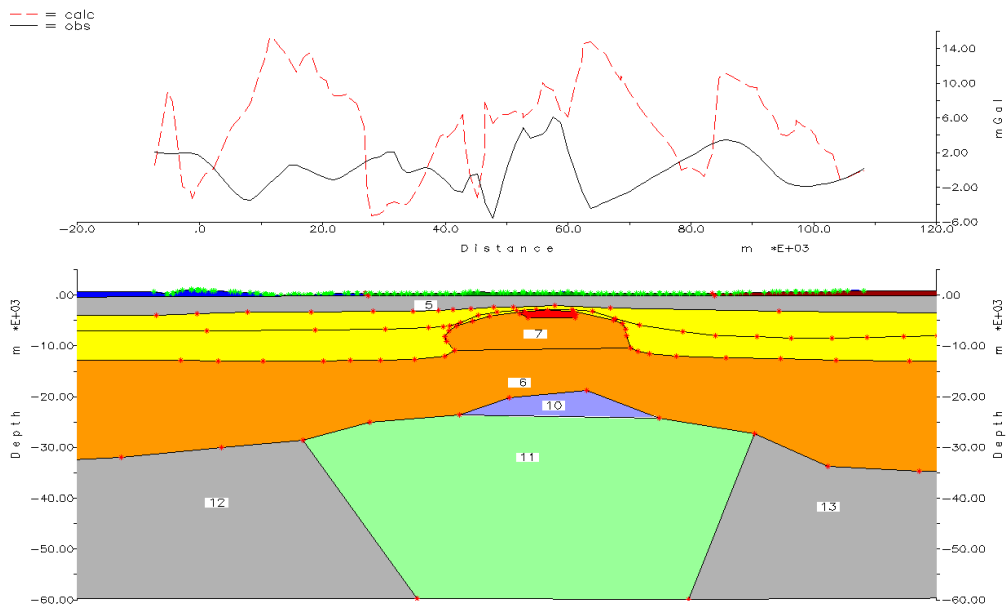
Fig. 6.8. *Forward 2.5-D gravity model 2 over Krafla caldera, according to Pálmason (1971) crustal seismic structure. Anomalous mantle is represented.*
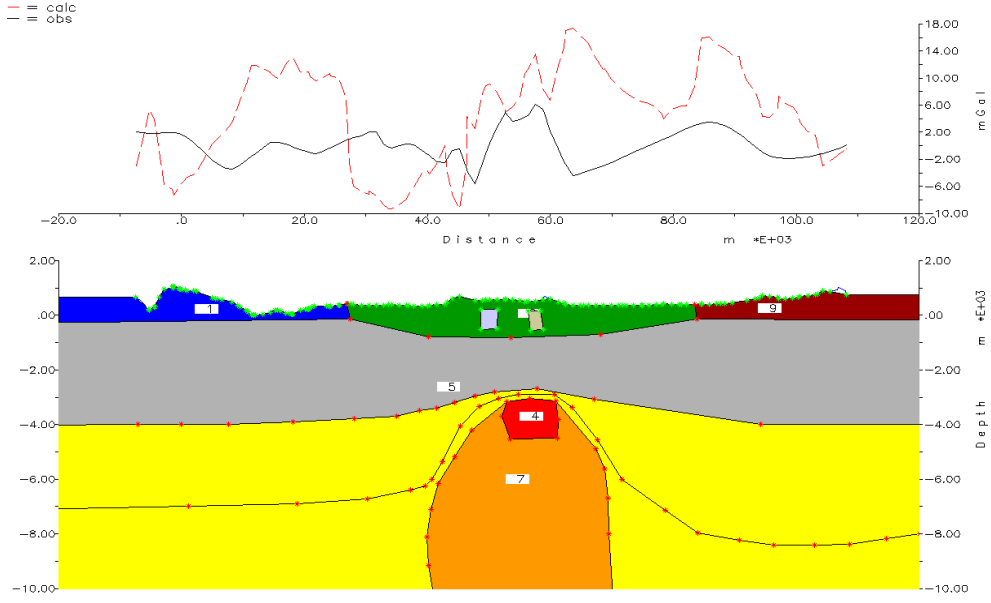
Model 3

Background density: 3.05 Mg/m^3. Layer 0 and 1=2.688, 2.015, 2.637. Layer 2 and 3 are the same. Layer 4: ρ_6=3.1, ρ_7=2.913. Mantle: $\rho_{10\&11}$=3.108, $\rho_{12\&13}$=3.23.

Fig. 6.9. Forward 2.5D gravity model 3 over Krafla caldera, using Pálmason (1971) crustal seismic structure. Zoom-in on the uppermost crustal layers and the high density bodies.

The seismic model of Pálmason according to this modeling is not consistent with the gravity model. Indeed large discrepancies are present. As in the case of Carlson and Herrick's (1980) systematic, the topography effect has a role in the discrepancies.

Some shallow bodies must be responsible for the observed gravity anomalies which are not present in the velocity model. The limiting depth method permits to determinate the maximum depth at which the top of the body could lie and still produce an observed gravity anomaly (Kearey *et al.*, 2002). We apply it on the central gravity high.

The gradient-amplitude ratio method requires the computation of the maximum anomaly amplitude (A_{max}) and the maximum horizontal gravity gradient (A'_{max}) (*Fig. 6.10*). For a three-dimensional body:

$$z < 0.86 \left| \frac{A_{max}}{A'_{max}} \right| \qquad (6.1)$$
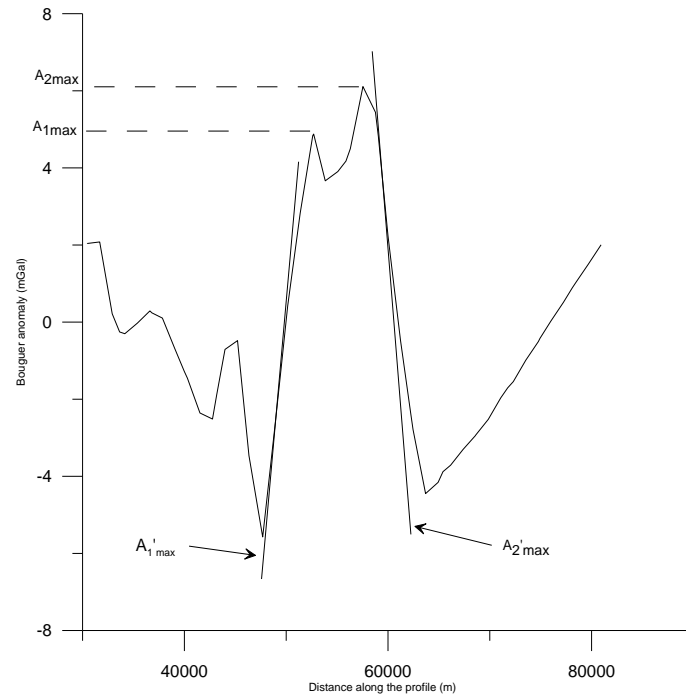
Fig. 6.6.10. *Limiting depths calculations using the half-width method on the central gravity high of Krafla volcano.*

The maximum horizontal gravity gradient is about 2.77 mgal/km for the first peak and 2.24 mGal/km for the second peak. Hence, $z_1 < 1.51$ km and $z_2 < 2.35$ km.

We can roughly estimate the thickness of these bodies from the density contrast ($\Delta\rho$) and the maximum gravity anomaly (Δg), using the Bouguer slab formula:

$$t \approx \frac{\Delta g}{2\pi G \Delta\rho}$$

(6.2)

If we consider a difference in density of 400 kg/m^3, we get

$$t_1 \approx t_2 \approx 615m$$

It seems interesting to add these 2 shallow high-density bodies for the last model. Proofs have been found, by Arnott and Foulger (1994) who identified ring structures and Árnasson *et al.* (2008) who infer a buried inner caldera.

6.3. Christensen and Wilkens (1982) systematic

From equation *(4.2)* and (*4.3*), the average density for each layer has been calculated. The initial parameters are seen in the following table.

Polygon	1	2	3	4	5	6 & 7	8	9
Density (Mg/m^3)	2,7	2,795	3,048	2,22	2,4	3,128	2,3	2,5

Table 3. *Model properties for Christensen and Wilkens(1982) systematic, used for gravity modeling with Gravmag software.*

Model 1

Background density: 2.964 Mg/m^3.
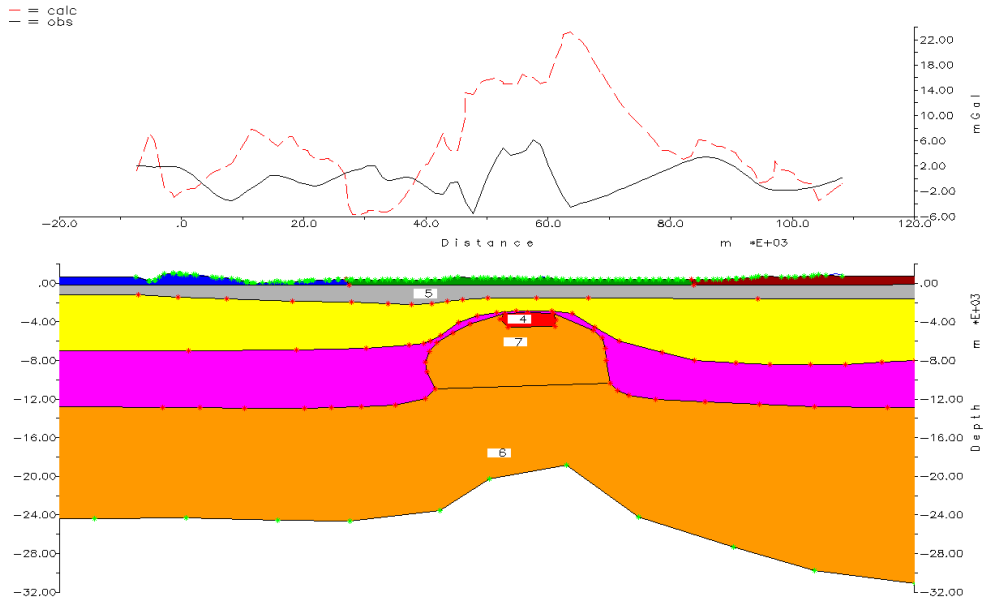
Fig. 6.11. *Forward 2.5-D gravity model 1 over Krafla caldera, according to Christensen and Wilkens (1982) systematic.*

Model 2

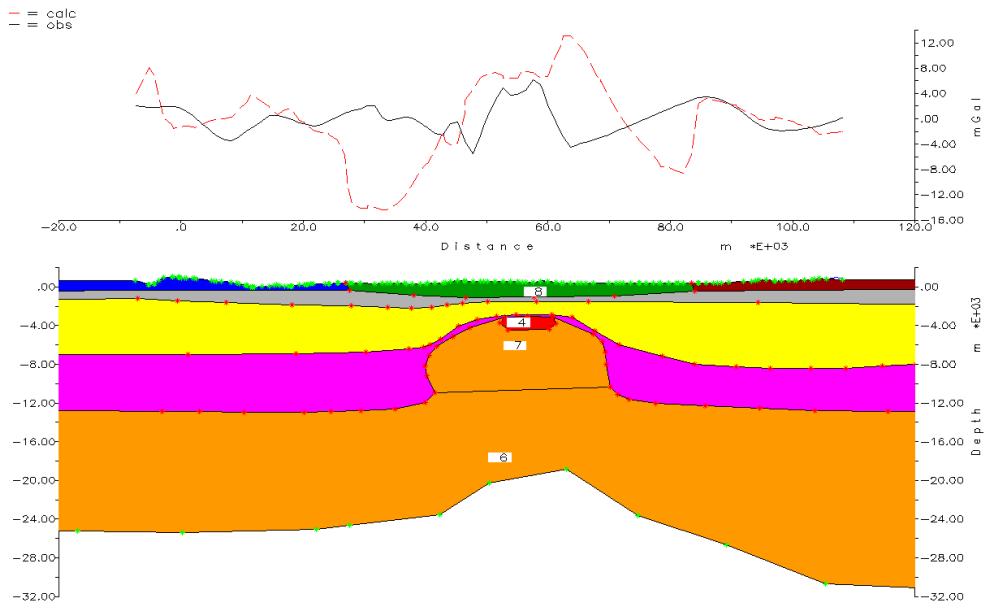Background density: 2.98 Mg/m^3. The properties of the surface layer have been optimized and the central part was made thicker. ρ_1=2.77, ρ_8=2.39; ρ_9=2.822.

Fig. 6.12. *Forward 2.5-D gravity model 2 over Krafla caldera, according to Christensen and Wilkens (1982) systematic.*

Model 3

Background density: 3.064 Mg/m^3. ρ_1=2.528, ρ_8=2.447, ρ_9=2.804, $\rho_{12\&13}$=3.23, $\rho_{10\&11}$=3.06.

The low-density mantle is added and the thicker crust as well. As for the previous models, the densities of the mantle are corrected from the one of Staples *et al.* (1997).
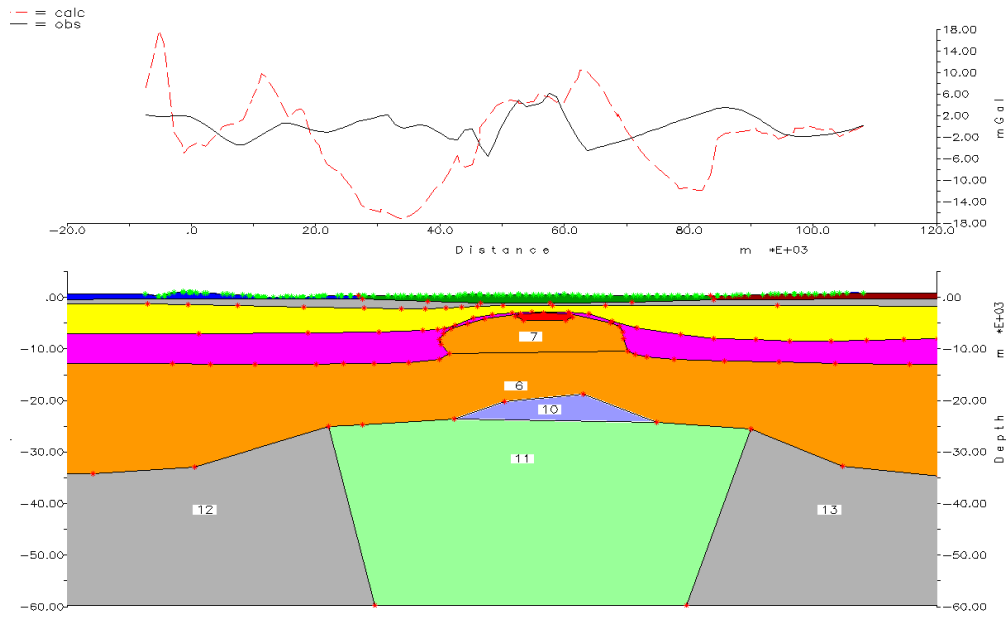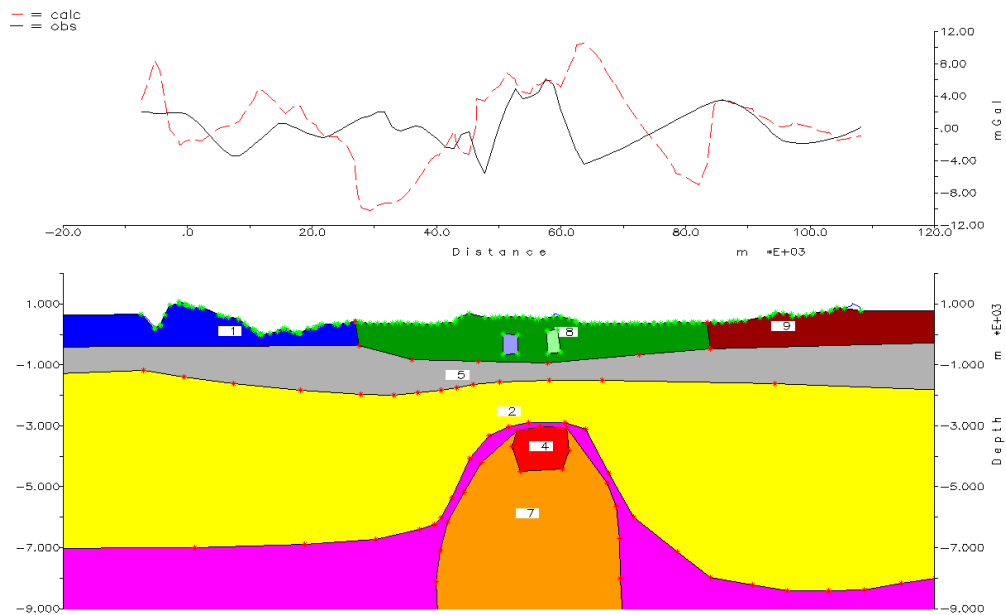
27

Fig. 6.13. *Forward 2.5-D gravity model 3 over Krafla caldera, according to Christensen and Wilkens (1982) systematic.*

Model 4

Background density: 2.96 Mg/m^3. ρ_1=2.723, ρ_8=2.417, ρ_9=2.819, ρ_6=3.133, ρ_7=2.973, ρ_{body1}=2.7, ρ_{body2}=2.6.

Fig. 6.14. *Forward 2.5-D gravity model 4 over Krafla caldera, according to Christensen and Wilkens (1982) systematic.*

On this zoom-in view *(fig. 6.14),* the two high-density bodies are seen. This layout gives the best fit with Christensen and Wilkens (1982) systematic. The two low anomalies are created by the boundary between the 3 polygons of the topographic layer. Apart from this discrepancy, the observed gravity field follows quite well the calculated one. The properties of the topographic layer polygons and those of the two bodies have been optimized thanks to Gravmag software.

7. DISCUSSION

All gravity models more or less show discrepancies concerning both the amplitude of the anomalies and the general shape. Christensen and Wilkens (1982) systematic seemingly gives better results than the two others. In each case, the dome has slightly slower velocity than predicted by the seismic model. The densities attributed to the surface layer are important as for the fit between observed and calculated gravity anomaly. Low densities coincide with the Krafla caldera, it is indeed filled with hyaloclastite. The existence of two shallow bodies in the models is justified by the anomalous ring structures found within the Krafla caldera by three geophysical methods: gravity data, seismic data and TM/MT data (Árnasson *et al.*, 2008). They probably represent intruded magma bodies. The boundaries of the magma chamber as mapped by Einarsson in 1978 and 1991 are still valid, the point source being at 2.8 km depth.

Although the relationships between velocity and density have been empirically found as approximately linear, the error margin can be quite large and thus the conversion is uncertain. For Pálmason's (1971) work the standard deviation and the error limit should be considered. Concerning Christensen and Wilkens (1982) systematic, the use of the equation (4.1) as the velocity/density relationship induces uncertainty too. For a given seismic velocity, the density may vary by up to ± 100 kg/m^3 from that predicted. Moreover, this relationship was established from Reydarfjörđur drillhole which is sited in tertiary rocks whereas Krafla area is in the neovolcanic zone and shows different rock types. In addition, this relation can only be used for velocities of 3.8 km/s or higher. Generally, all relations can be used for velocities of 2.5 km/sec or higher.

There is also an uncertainty in the data. The topography profile has been drawn by hand and the topography estimated from a topographic map. The shape of bodies is also uncertain but does not really influence the gravity field. The interest is in the variations, and in the influence of density contrast and configuration of the causative bodies. As for the removal of regional field, instead of the linear trend, we could use the value of 0.5 mgal/km for the regional gradient in the area (Schleusener *et al.,* 1976). It could be interesting to do an upward continuation of the Bouguer anomaly in order to attenuate the high-wavenumber anomalies and enhance the anomalies of the deeper-seated sources. This process allows determining the form of regional gravity variation over a survey area (Kearey *et al.,* 2002). Indeed, the anomalies are most likely caused by bodies at different depths. Anomalies originate from density variations at very shallow depth so most of the small changes cannot be modeled.

The average elevation of the Krafla area being about 500 m a.s.l., the Bouguer slab is about 500 m thick. The Bouguer correction assumes this slab to have a uniform density. However, rock types are in reality highly diverse especially at the surface, as a result of intensive volcanic activity and this may result in errors in the Bouguer anomaly of up to about 1 mGal (Foulger and Field, 2000). For verification, rock samples should be collected and estimation of density made, for example weighing them in the air and water.

Finally, a gravity profile in a perpendicular direction would allow a 3D modeling of the magma chamber beneath the Krafla caldera. The use of three-dimensional crustal structure may significantly improve the resolution of structures as shown by Arnott and Foulger (1994) in their velocity model.

8. CONCLUSION

In this project, I performed a comparison between the gravity and seismic anomalies. Indeed, Gravity data can be used to test a velocity model determined by seismic refraction. When the seismic data are combined with gravity data, the average densities of rocks at various depths can be obtained (Pálmason, 1971). Concerning the Krafla gravity modeling, it demonstrates that the seismic models do not show all the information about the subsurface structure of the volcano. The fact that the gravity field is mostly sensitive to very shallow structures explains the discrepancies. Krafla being volcanically active, there are a lot of shallow heterogeneities. There are lateral variations in density in the Krafla area. The basaltic intrusions that underlie the caldera fill may be elevated to a depth of 400-500 m b.s.l. within the caldera, compared with about 1000m b.s.l. just south of the caldera (Ármannsson *et al.,* 1987). This explains the velocity/density high observed in the center of the caldera.

Finally it is necessary to correlate the data to find out and interpret the density contrasts and the layout of the different bodies. The same observations are made for the continental crust. Barton (1986) studied the relationship between seismic and gravity anomalies in the continental crust. He concluded that the use of a seismic velocity measurement as the only indication of rock density does not provide a useful constraint when attempting to reproduce observed gravity variations.

It is interesting to compare the case of Krafla with other Icelandic volcanoes. In the Vatnajökull region Bárðarbunga, Kverkfjöll and Grímsvötn are large central volcanoes that have also been associated with major density anomalies located in the upper crust. It corresponds to high density bodies located between 1 and 5 km depth. The assumption is the same as for Krafla, these bodies being gabbroic cumulates from an overlying magma chamber. At Grímsvötn the magma chamber has been inferred from ground deformation. The gravity highs associated with the caldera faults of these three volcanoes come from upwards protrusions from the high density bodies (Gudmundsson and Högnadóttir, 2006), similarly to Krafla. Askja volcano is located 80 km to the south of Krafla volcanic system and is also experiencing magma drainage from a shallow reservoir. A link between the two volcanoes is suggested by Tryggvason (1986, 1993) and Sturkell *et al.* (2004). They might be interconnected at depth and a pressure-link between these volcanoes might exist along the ductile lower crust in Iceland. De Zeeuw-van Dalfsen *et al.* (2006) suggested the existence of deep magma accumulation at 21 km depth in addition to the magma reservoir at 2.8 km depth.

The knowledge of the crustal structure of Krafla is useful in many different senses. Krafla volcanic system is still subject to deformation, because of stresses associated with the divergent plate boundary, the effects of magma movements and geothermal processes (de Zeeuw-van Dalfsen *et al.,* 2006) which are cooling the volcanic system. Currently deflating, Krafla volcano will probably experience another rifting event within hundreds of years. The power plant using its geothermal fields has an important role. It is necessary to know the effect of extensive exploitation of geothermal resources - Landsvirkjun planning to expand the power generation in the Krafla geothermal field. Moreover, Krafla is one of few calderas in the world and it is more accessible than Askja central volcano to study. Crustal magma chambers play a major role in crustal genesis at the plate boundary (Brandsdóttir *et al.,* 2008). Using a range of geophysical techniques will therefore broaden our knowledge of the processes taking place in Iceland at active volcanoes.

ACKNOWLEDGMENTS

REFERENCES

Ármannsson, H., A. Guðmundsson, and B.S. Steingrimsson 1987. Exploration and development of the Krafla geothermal area. *Jökull* 37, 13-30.

Árnason, K., A. M. Vilhjálmsson and Þ. Björnsdóttir 2008. A study of the Krafla volcano using gravity, micro earthquake and MT data. ISOR Iceland GeoSurvey, prepared for Landsvirkjun.

Arnott, S.K., and G.R. Foulger, 1994. The Krafla spreading segment, Iceland.1. Three-dimensional crustal structure and the spatial and temporal distribution of local earthquakes. *J. Geophys. Res.* 99, 23,801-23,825.

Barton, P.J. 1986. The relationship between seismic velocity and density in the continental crust — a useful constraint? Geophysical Journal of the Royal Astronomical Society Vol. 87, 195-208.

Bath, M. 1960. Crustal structure of Iceland. *J. Geophys. Res.* 65, 1793-1807.

Brandsdóttir, B., W.H. Menke, P. Einarsson, R. White and R. Staples 1997. Färoe-Iceland Ridge Experiment. *J. Geophys. Res.* 102, 7849-7886.

Brandsdóttir, B. and W.H. Menke 2008. The seismic structure of Iceland. *Jökull* 58, 17-34.

Carlson, R.L., and C.N. Herrick 1990. Densities and Porosities in the Oceanic Crust and Their Variations With Depth and Age. *J. Geophys. Res.* 95, 9153-9170.

Christensen, N.I. and R.H. Wilkens 1982. Seismic properties, Density, and composition of the Icelandic Crust Near Reydarfjordur. *J. Geophys. Res.* 87, 6389-6395.

Darbyshire, F.A., R.S. White, and K.F. Priestley 2000. Structure of the crust and uppermost mantle of Iceland from a combined seismic and gravity study. *Earth and Planetary Science* Letters 181, 409-428.

Einarsson, P. 1978. S-wave shadows in the Krafla caldera in NE-Iceland, evidence for a magma chamber in the crust. *Bull. Volcanol.* 41,1-9.

Foulger, G.R. and P.R. Field 2000. Comparison of local earthquake tomographic crustal models with gravity data for the Hengill-Grensdalur and Krafla areas. *Jokull* 48, 29-47.

Gudmundsson, M.T. and T. Högnadóttir 2006. Volcanic systems and calderas in the Vatnajökull region, central Iceland: Constraints on crustal structure from gravity data. *J. of Geodynamics* 43 (2007), 153-169.

Ier, H.M., 1984. Geophysical Evidence for the Locations, Shapes and Sizes, and Internal Structures of Magma Chambers beneath Regions of Quaternary Volcanism. *Philosophical Transactions of the Royal Society of London. Series A, Mathematical and Physical Sciences* 310, 473-510.

Johannesson, H. and Sæmundsson, K., 1998. Geological Map of Iceland. 1:500000. Bedrock Geology. Icelandic Institue of Natural History, Reykjavik (2nd edition).

Johnsen, Gunnar V. 1995. Pyngdarkort af Kröflusvaedi, in: *EYJAR I ELDHAFI*, ed. Björn Hroarsson, Dagur Jonsson and Sigurdur Sveinn Jonsson, Gott nal hf., 93-100.

Kearey, P., M. Brooks and I. Hill 2002. An Introduction to Geophysical Exploration, 3rd Edition. Wiley-Blackwell. ISBN: 978-0-632-04929-5.

Pálmason, G., Crustal Structure of Iceland from Explosion Seismology 1971. *Visindaelag Islendiga*, 187 pp.

Pedley, R.C., J.P. Busby and Z.K. Dabek 1993. GRAVMAG User Manual – Intereactive 2.5D gravity and magnetic modeling. *British Geological Survey, Technical Report WK/93/26/R*.,73pp.

Rymer, H., J. Cassidy, C.A. Locke, F. Sigmundsson 1998. Post-eruptive gravity changes from 1990 to 1996 at Krafla volcano, Iceland. *J. Volcanol. Geotherm. Res.* 87, 141-149.

Sæmundsson K. 1979. Outline of the geology of Iceland. *Jökull* 29, 7-28.

Sæmundsson K. 1991. Jarðfræði Kröflusvæðisins, in: *Nattura Myvatns*, ed. Arnpor Gardaarsson and Arni Einarsson, 24-95.

Schleusener A, W. Torge, and H. Drewes 1976. Gravity field of Northeastern Iceland. *J. Geophysics* 42, 27-45.

Staples, R.K., R.S. White, B. Brandsdóttir, W. Menke, P.K.H. Maguire, and J.H. McBride 1997. Faroe-Iceland Ridge Experiment- Crustal structure of northeastern Iceland. *J. Geophys. Res.* 102, 7849-7866.

Sturkell, E., F. Sigmundsson, H. Geirsson, H. Olafsson, T. Theodorsson 2008. Multiple volcano deformation sources in a post-rifting period: 1989-2005 behaviour of Krafla, Iceland constrained by leveling, tilt and GPS observations. *J. Volcanol. Geotherm. Res.* 177, 405-417.

Thordarson, T., and A. Höskuldsson 2002. Iceland; *Classic Geology in Europe 3*. Harpenden, U.K. Terra publishing, 200p.

Tryggvason E., 1986. Multiple magma reservoirs in a rift zone volcano: ground deformation and magma transport during the September 1984 eruption of Krafla, Iceland. *J. Volcanol. Geotherm. Res.* 28, 1-44.

De Zeeuw-van Dalfsen, E., H. Rymer, G. Williams-Jones, E. Sturkell, and F. Sigmundsson 2006. *Bull. Volcanol.* 68, 420-431.

Topographic map of Iceland, surveyed by the Geodetic Institute Copenhagen 1932-34, Revised by "Landmaelingar Islands" 1969. 1:250000.

Conversion of UTM coordinate using an Excel spreadsheet from Steven Dutch, Natural and Applied Sciences, University of Wisconsin - Green Bay.

APPENDIX- GRAVITY DATA